Synthesis and characterization of thiolated carboxymethyl chitosan-graft-cyclodextrin nanoparticles as a drug delivery vehicle for albendazole

Ghazaleh Alamdarnejad, Alireza Sharif, Shahrouz Taranejoo, Mohsen Janmaleki, Mohammad Reza Kalaee, Mohsen Dadgar & Mazyar Khakpour

Journal of Materials Science: Materials in Medicine
Official Journal of the European Society for Biomaterials

ISSN 0957-4530

J Mater Sci: Mater Med
DOI 10.1007/s10856-013-4947-9

Springer

J Mater Sci: Mater Med
DOI 10.1007/s10856-013-4947-9

Synthesis and characterization of thiolated carboxymethyl chitosan-graft-cyclodextrin nanoparticles as a drug delivery vehicle for albendazole

Ghazaleh Alamdarnejad · Alireza Sharif · Shahrouz Taranejoo · Mohsen Janmaleki · Mohammad Reza Kalaee · Mohsen Dadgar · Mazyar Khakpour

Received: 4 November 2012 / Accepted: 29 April 2013

Abstract A new strategy for the synthesis of thiolated carboxymethyl chitosan-g-cyclodextrin nanoparticles by an ionic-gelation method is presented. The synthetic approach was based on the utilization of 1,6-hexamethylene diisocyanate during cyclodextrin grafting onto carboxymethyl chitosan. The use of the 1,6-hexamethylene diisocyanate resulted in reactions between cyclodextrin and active sites at the C_6-position of chitosan, and preserved amino groups of chitosan for subsequent reactions with thioglycolic acid, as the thiolating agent, and tripolyphosphate, as the gelling counterion. Various methods such as scanning electron microscopy, rheology and in vitro release studies were employed to exhibit significant features of the nanoparticles for mucosal albendazole delivery applications. It was found that the thiolated carboxymethyl chitosan-g-cyclodextrin nanoparticles prepared using an aqueous solution containing 1 wt% of tripolyphosphate and having 115.65 (μmol/g polymer) of grafted thiol groups show both the highest mucoadhesive properties and the highest albendazole entrapment efficiency. The latter was confirmed theoretically by calculating the enthalpy of mixing of albendazole in the above thiolated chitosan polymer.

Electronic supplementary material The online version of this article (doi:10.1007/s10856-013-4947-9) contains supplementary material, which is available to authorized users.

G. Alamdarnejad
Young Researchers Club, South Tehran Branch, Islamic Azad University, Tehran, Iran

A. Sharif (✉)
Faculty of Chemical Engineering, Department of Polymer Engineering, Tarbiat Modares University, P.O. Box: 14155/143, Tehran, Iran
e-mail: asharif@modares.ac.ir

S. Taranejoo · M. Janmaleki
Medical Nanotechnology and Tissue Engineering Research Center, Shahid Beheshti University of Medical Sciences, Tehran, Iran

M. R. Kalaee
Department of Polymer Engineering, Islamic Azad University, South Tehran Branch, Tehran, Iran

M. Dadgar
Faculty of Applied Chemistry, Islamic Azad University, South Tehran Branch, Tehran, Iran

M. Khakpour
Department of Polymer Engineering, Islamic Azad University, Kashan Branch, Kashan, Iran

1 Introduction

Hydrophobic drugs comprise a very important class of therapeutic agents which are of great potential use in treatment of cancer and helminth infections [1, 2]. Unfortunately, these pharmaceuticals have achieved limited success in clinical applications because of the difficulties in oral and intravenous administrations caused by low drug solubility in aqueous media, rapid hydrolysis and enzymatic degradation. Several methods have been investigated to overcome these deficiencies, including the use of various drug carriers such as micelles [3], hydrogels [4, 5], microparticles [6, 7], nanoparticles [8, 9], etc. Among these drug delivery vehicles, the systems based on chitosan are of great interest due to their good biocompatibility, prolonged drug release behavior and non-toxicity [10–13]. Since, modification of chitosan, as a poor soluble and weakly interacting polysaccharide, is a critical prerequisite for its conjugation to hydrophobic drugs, considerable efforts have been devoted to address this issue in recent years. For

Published online: 12 May 2013

example, Anitha et al. [14] reported a simple method of solvent evaporation followed by ionic-gelation to develop nanoparticles based on carboxymethyl chitosan (CMC) for controlled delivery of anticancer drugs. Also, Molnar et al. [15] prepared a series of *O*-substituted alkylglyceryl chitosan nanoparticles with systematically varied degrees of grafting as materials for the formulation of colloidal systems that could act as drug carriers into the brain. In another investigation, a pH- and thermo-responsive chitosan-graft-poly(*N*-vinylcaprolactam) (PNVCL) copolymer was reported as the base material for preparation of a device for controlled delivery of a hydrophobic drug, ketoprofen [16]. Due to the presence of PNVCL chains, the copolymer showed a temperature-induced phase transition at 32 °C in an aqueous medium, leading to the controlled release of the drug into the medium.

β-cyclodextrin (β-CD)-linked chitosan has also been investigated by a few groups and found to be an efficient carrier for the controlled delivery of hydrophobic drugs [17, 18]. Cyclodextrins (CDs) are cup-shaped molecules with hydrophobic cavities and hydrophilic exteriors, and have the ability to interact with various hydrophobic guest molecules to form supramolecular inclusion complexes [19, 20]. They have been exploited to enhance the bioavailability of insoluble drugs by increasing the drug solubility and permeability. Moreover, the safety of CDs in humans has been well established [19, 21].

Prabaharan and Gong [22] coupled cysteine methyl ester hydrochloride (CMEH) to carboxymethyl chitosan-g-β-cyclodextrin (CMC-*g*-β-CD) by a 1-ethyl-3-(3-dimethylaminopropyl) carbodiimide (EDC) mediated reaction to form mucoadhesive carriers for hydrophobic drug delivery. Although the resultant carriers showed an appropriate drug release profile, the large particle size (in micrometer size range) and rather broadened size distribution were unfavourable for their application in nanomedicine. Due to these limitations the prepared carriers did not have the ability to access different areas of the human body such as the mucosal layer.

The present study aimed to develop a new synthetic route to yield nanoparticles, composed of thiolated carboxymethyl chitosan-g-cyclodextrin, as efficient mucoadhesive systems for controlled delivery of hydrophobic drugs. To this end, β-cyclodextrin was grafted onto carboxymethyl chitosan (CMC) in the presence of 1,6-hexamethylene diisocyanate (HMDI) reagent, acting as a spacer between the cyclodextrin and CMC. Accordingly, amino groups at the C_2-position of chitosan remained free to form amide bonds with thioglycolic acid (TGA), as the thiolating agent, and to react with sodium tripolyphosphate (TPP), as the gelling counterion, during the nanoparticles formation. The prepared nanoparticles were physicochemically characterized by different methods including X-ray diffraction (XRD), scanning electron microscopy (SEM), thermogravimetric analysis (TGA), differential scanning calorimetry (DSC) and rheology. Also, in vitro release of albendazole (ABZ), as a hydrophobic antiparasitic as well as anticancer drug [23, 24], from the nanoparticles was studied.

2 Materials and methods

2.1 Materials

Chitosan (M_w = 300,000 g/mol, 85 % deacetylated), β-cyclodextrin, Ellman's reagent (DTNB, 5,5′-dithiobis (2-nitrobenzoic acid)) and stannous 2-ethylhexanoate were purchased from Aldrich and used as received. HMDI, *N*,*N*-dimethylformamide (DMF), TPP, TGA and EDC, were obtained from Merck (Germany). Mucin from porcine stomach (Type II) was supplied from Sigma. Albendazole was a generous gift from Damloran Co. (Iran). All other chemicals used were of analytical reagent grades.

2.2 Synthesis of *O*-carboxymethyl chitosan (CMC)

In order to synthesis of CMC, 1.5 g of the chitosan sample was added into 1 mL of an aqueous solution containing 50 wt% of sodium hydroxide (NaOH) and the mixture was placed in a refrigerator (−18 °C) for 48 h for alkalization. After the excessive alkali solution was extruded, chitosan was mixed in 10 mL of isopropyl alcohol and then chloroacetic acid was added to the mixture dropwise. This mixture was stirred at room temperature for 2 h followed by stirring at 60 °C for another 2 h. The final solution was neutralized by chloridric acid (HCl) and dialyzed in tubing (molecular weight cutoff 12 kDa) against distilled water for 3 days to remove the impurities and unreacted materials. The resultant product, CMC, was freeze dried and stored at room temperature [22].

2.3 Grafting β-cyclodextrin onto CMC

In brief, 1 g of the prepared carboxymethyl chitosan was dissolved in 1 mL of a solution containing 5 % (v/v) of HMDI in toluene. After adding few drops of stannous 2-ethylhexanoate as a catalyst, the mixture was magnetically stirred at room temperature for 45 min to ensure complete reaction between the CMC and HMDI. Subsequently, the supernatant was discarded and HMDI-grafted CMC (CMC-HMDI) was dissolved in a solution containing 2 % (w/v) of the β-CD in DMF. The solution was magnetically stirred for 1 h at room temperature, after adding few drops of the stannous 2-ethylhexanoate catalyst, which resulted in reactions between isocyanate groups of the

CMC-HMDI, and β-CD [25]. The supernatant was decanted and the obtained carboxymethyl chitosan-g-cyclodextrin (CMC-CD) was washed several times with deionized water and ethanol, separately, and finally freeze dried.

2.4 Grafting TGA onto CMC-CD

Thiolated carboxymethyl chitosan-g-cyclodextrin (TGA-CMC-CD) was prepared by covalent attachment of thioglycolic acid to the primary amino groups of CMC-CD following the method described by Saboktakin et al. [26]. In brief, the CMC-CD was dissolved in 1 % acetic acid solution; thereafter EDC dissolved in 1 mL demineralized water was added to a final concentration of 125 mM. Different amounts of thioglycolic acid were then added and the reaction mixture was incubated for 3 h at room temperature under vigorous stirring. The synthesis was performed at pH 5.0, in order to avoid the formation of disulfide bonds between the polymer chains during the coupling reaction. Unbound compounds were isolated by exhaustive dialysis for five times and the product was lyophilized by freeze drying and kept at 4 °C for further use. The synthesis route of the TGA-CMC-CD is presented in Scheme 1. The optimal conditions to achieve TGA-CMC-CD's containing the highest amount of coupled thiol groups, resulting in improved mucoadhesive properties [27], were determined by central composite design (CCD). According to the CCD methodology, two TGA-CMC-CD samples, referred to as TGA-CMC-CD(1) and TGA-CMC-CD(2), containing 115.65 and 91.56 (μmol/g polymer) of thiol groups, respectively, were synthesized and used for

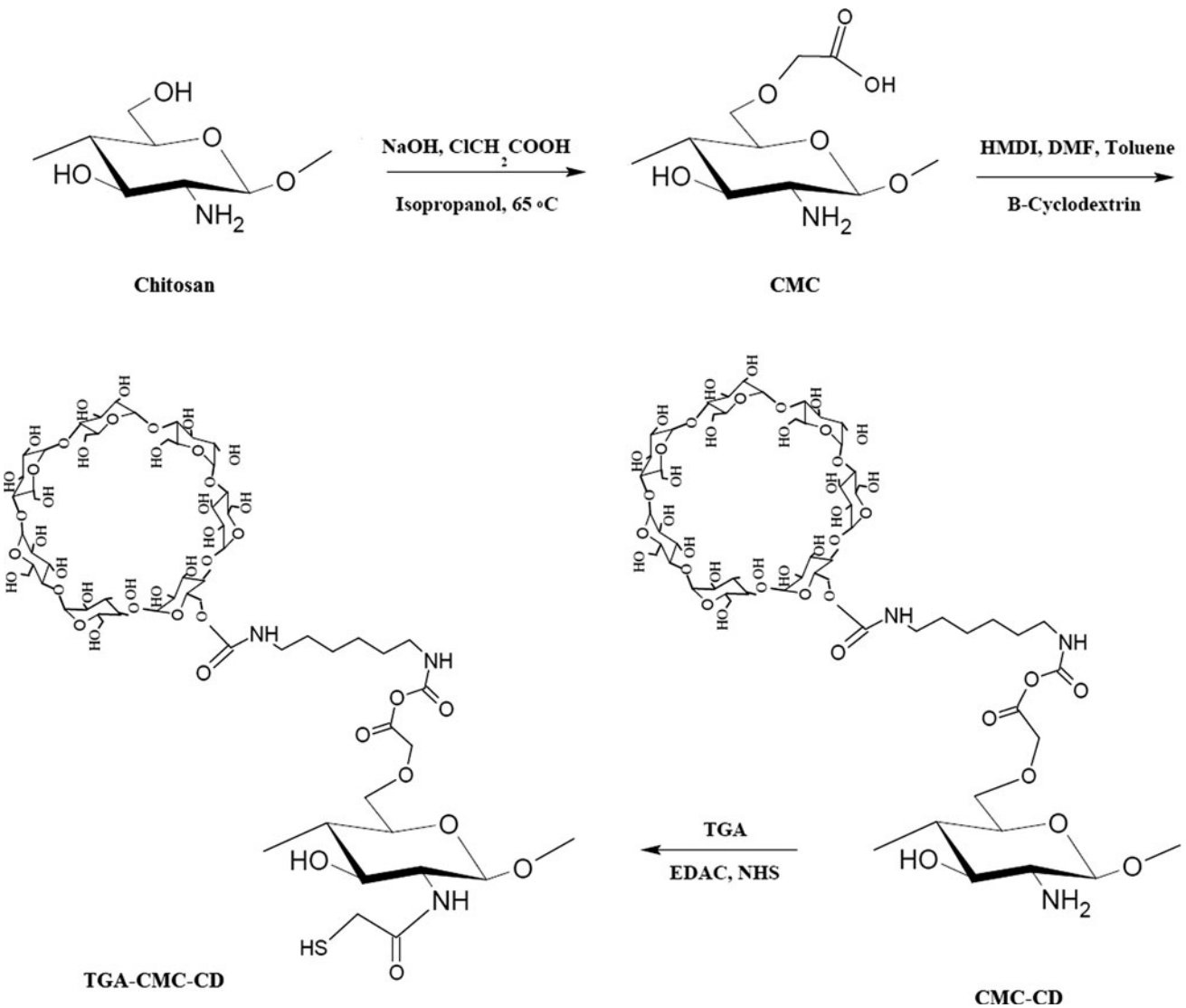

Scheme 1 Modification of chitosan and formation of thiolated carboxymethyl chitosan-g-cyclodextrin (TGA-CMC-CD) polymer

further analysis. Details of the experimental design can be found in Online Resource 1.

2.5 Determination of thiol group content

The amount of grafted thiol groups on the prepared TGA-CMC-CD polymers was evaluated using Ellman's reagent. A 2 mg/mL solution of the polymer was prepared in distilled water. Afterward, 250 µl aliquots of this solution were added to 250 µl of 0.5 mol/L phosphate buffer (PBS), pH 8.0, and to 500 µl of the Ellman's reagent (0.3 mg/mL of DTNB in 0.5 mol/L PBS, pH 8.0) (final polymer concentration of 0.5 mg/mL). The reaction was allowed to proceed for 2 h at room temperature and the absorbance was measured by a UV/Visible spectrophotometer (Super Aquarius UV/Visible spectrophotometer Cecil, CE9200, England) at a wavelength of 420 nm. Control samples were elaborated with non-modified chitosan. The amount of thiol moieties was calculated from the corresponding standard curve elaborated between 0.25 and 2 mol/L of thioglycolic acid–water. All experiments were performed in triplicate [28].

2.6 Preparation of albendazole loaded nanoparticles

In order to prepare drug loaded nanoparticles, 100 mg of albendazole along with 200 mg of each of the polymers: chitosan, CMC-CD or TGA-CMC-CDs, were dissolved in 50 mL acetic acid (50 % v/v in water), under vigorous stirring for 24 h, at room temperature. Afterward, 1 mL of an aqueous solution containing 1 wt% of TPP was added dropwise to 10 mL of the drug–polymer solution, while it was kept in an ultrasonic bath (25 °C). After 30 min, the resultant albendazole loaded nanoparticles were collected by centrifugation at 13,200 rpm for 1 h, washed in deionizer water, redispersed in distilled water and finally lyophilized. The amount of the albendazole remaining in the supernatant was analyzed using the UV–Visible spectrophotometer at a wavelength of 291 nm.

The drug entrapment efficiency (EE) can be obtained according to the following equation:

$$EE(\%) = \frac{A - B}{A} \times 100\% \quad (1)$$

where A is the total amount of albendazole and B is the amount of albendazole remaining in the supernatant.

The neat chitosan, CMC-CD and TGA-CMC-CD nanoparticles (albendazole free nanoparticles) were also prepared under the same conditions, for comparison. Furthermore, in order to investigate the effect of TPP concentration on the size and morphology of the nanoparticles, aqueous solutions containing different concentrations of TPP (0.25, 0.5, 1 and 2 wt%) were used for the preparation of neat TGA-CMC-CD nanoparticles.

2.7 Mucoadhesive properties measurements

Mucoadhesive properties of the thiolated and un-thiolated nanoparticles were examined by rheological experiments. Approximately 4 mg of each nanoparticle sample was first dispersed in 1 mL of demineralized water under vigorous stirring. Afterward, 500 µg of the mucin powder, dispersed in 1 mL demineralized water (pH 7.4), was added to the nanoparticle/water solution and the resultant mixture was incubated for 1 h at 37 °C. Finally, 1 mL of the nanoparticle/mucin mixture was transferred to a cone and plate viscometer (RheoPlus MCR300 SN599139) and allowed to equilibrate on the plate for 3 min at 37 ± 0.5 °C. Frequency sweep measurements were carried out in a frequency range of 0.1–10 Hz.

2.8 Calculation of solubility parameters using the group contribution method

The partial solubility parameters (δ_d, δ_p and δ_h), of albendazole, chitosan and the synthesized chitosan derivatives (CMC-CD and TGA-CMC-CD) were computed using the group contribution method according to the following equations [29]:

$$\begin{aligned} \delta_d &= \sum F_{di}/V \\ \delta_p &= \left(\sum F_{pi}^2\right)^{0.5}/V \\ \delta_h &= \left(\sum E_{hi}\right)^{0.5}/V \end{aligned} \quad (2)$$

where F_{di}, F_{pi} and E_{hi} denote, the functional group contributions of dispersion forces (d), dipole/dipole interactions (p) and hydrogen bonding (h), respectively. The total molar volumes (V) of the drug and repeating units of the polymers (Scheme 1) were obtained according to the method proposed by van Krevelen [29]. Subsequently, the enthalpy of mixing (ΔH_m, MPa) of components 1 and 2 of each polymer(1)/drug(2) mixture can be represented as [30]:

$$\Delta H_m = \Phi_1 \Phi_2 \left[(\delta_{d1} - \delta_{d2})^2 + (\delta_{p1} - \delta_{p2})^2 + (\delta_{h1} - \delta_{h2})^2 \right] \quad (3)$$

where Φ_1 and Φ_2 are the volume fractions of polymer and drug, respectively.

2.9 In-vitro release studies

In-vitro release of albendazole from the chitosan-based nanoparticles was studied in a glass apparatus containing 50 mL of a buffered saline solution (PBS, pH 7.4), as the release medium, at 37 °C. This medium is very similar to human intestinal fluid. For this purpose, 10 mg of the

albendazole-loaded nanoparticles were suspended in the medium and kept in a horizontal laboratory shaker, maintaining constant temperature and stirring (300 rpm). Samples (5 mL) were periodically removed and the volume of each sample was replaced by the same volume of fresh medium. The amount of the released albendazole was analyzed by the UV-spectrophotometer at 291 nm. The drug-release studies were performed in triplicate for each of the samples.

3 Characterization

Fourier transform Infrared (FTIR) spectra of the chitosan, CMC, CMC-CD and TGA-CMC-CD were recorded with a Tensor^{TM} 27 Bruker spectrophotometer, Germany, in the range of 4,000–400 cm^{-1}. X-ray diffraction (XRD) patterns of the samples were obtained using an X-ray diffractometer (X'Pert MPD model, Philips, Holland) equipped with Cu Kα. The tube was operated at 40 kV, 30 mA. Differential scanning calorimetry and thermogravimetric analysis (DSC/TGA) of the chitosan and TGA-CMC-CD samples were performed using an STA-1500 (Sinco, Korea) instrument. The apparatus was calibrated with purified indium (99.9 %). Samples were placed in flat-bottomed aluminium pan and heated at a constant rate of 10 °C/min in an atmosphere of nitrogen in a temperature range of 30–300 °C. Furthermore, the morphology of the chitosan, CMC-CD and TGA-CMC-CD nanoparticles were determined by field emission scanning electron microscopy (FE-SEM, Philips XL30, 15 kV voltage). All the samples were sputter-coated with a thin layer of gold before imaging. The particle size and size distribution of the nanoparticles were determined using ImageJ 1.42q and PASW Statistics 18 softwares, respectively.

4 Results and discussions

4.1 Chitosan modification

Figure 1 represents the FTIR spectra of chitosan, CMC, CMC-CD and TGA-CMC-CD(1) samples. The FT-IR spectrum of chitosan showed a broad −OH stretching absorption band between 3,500 and 3,100 cm^{-1}. The peak around 1,640 cm^{-1} represented acetylated amino groups of chitin, which indicated that the sample was not fully deacetylated. The peak at 1,370 cm^{-1} corresponded to the −C–O stretching of primary alcoholic groups (−CH_2−OH). Also, the absorption peaks at 659 and 1,558 cm^{-1} were related to amino (−NH_2) groups of chitosan. In the IR spectrum of CMC, the strong peaks at 1,560 and 1,415 cm^{-1} were assigned to the respective asymmetry and

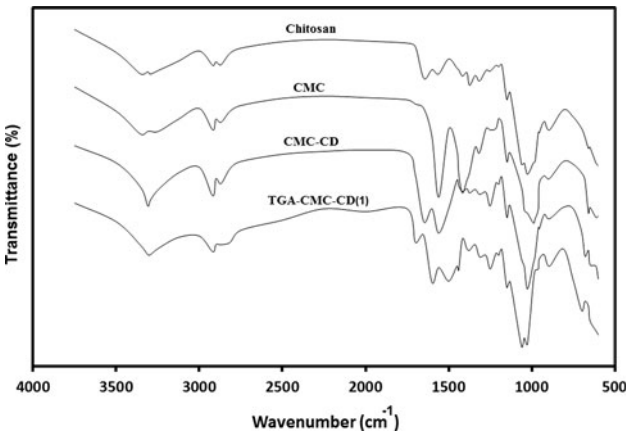

Fig. 1 FTIR spectra of chitosan, CMC, CMC-CD and TGA-CMC-CD(1) samples

symmetry stretching vibration of COO^-. These results indicated that the carboxymethyl substitution occurred at the C_6-position of chitosan [22]. The peaks at 1,650 and 950 cm^{-1} in the FTIR spectrum of CMC-CD, could be assigned to the stretching vibration of carbonyl groups and α-pyranyl vibration of β-CD, respectively. Moreover, the OH bending band, appeared as a weak shoulder at 3,290 cm^{-1} in the spectra of the chitosan and CMC, were not observed in that of the CMC-CD, implying that most of the hydroxyl groups of CMC reacted with isocyanine (–NCO) groups of the HMDI. The FTIR spectrum of TGA-CMC-CD(1) shows all the characteristic peaks of CMC-CD, except the peaks corresponding to amino (−NH_2) groups, suggesting that amino groups of CMC-CD were reacted with carboxyl groups of thioglycolic acid. This resulted in new amide bonds with characteristic peaks at 1,500 and 1,629 cm^{-1}. However, as it was mentioned in Sect. 2.4, the amount of grafted thiol groups on the TGA-CMC-CD(1) sample was found to be 115.65 (μmol/g polymer). Therefore, the amount of free amino groups of TGA-CMC-CD(1), needed for the formation of nanoparticles, was calculated as 0.837 (μmol/g polymer), considering the structure of the repeating unit of a TGA-CMC-CD molecule, Scheme 1. Consequently, the disappearance of the characteristic peaks of free amino groups in the FTIR spectrum of TGA-CMC-CD(1) could be attributed to the insensitivity of FTIR method to detect such a low concentration of these groups. Furthermore, the absorption band at 1,700 cm^{-1} in the spectrum of TGA-CMC-CD(1) was ascribed to the carbonyl groups of TGA molecules.

To identify the crystallinity of TGA-CMC-CD(1), its XRD pattern is compared with that of the chitosan in Fig. 2. Chitosan powder showed two major broad crystalline peaks at 2θ around 10° and 20°, respectively, whereas the intensities of these peaks were significantly decreased in the XRD pattern of TGA-CMC-CD(1). Therefore, one

can conclude that the chemical modification could destroy the crystalline structure of chitosan, leading to the TGA-CMC-CD(1) polymer with a more amorphous structure and higher biodegradability and mucoadhesive properties [22].

The DSC/TGA curves of chitosan and TGA-CMC-CD(1) are presented in Fig. 3a, b. Chitosan and TGA-CMC-CD(1) showed characteristic endothermic peaks around 90 and 80 °C, respectively, corresponding to the evaporation of bound water as well as exothermic peaks at 285 and 260 °C, respectively, due to the samples decomposition (Fig. 3a). The endothermic peak of chitosan was broader than that of the TGA-CMC-CD(1), due to the fact that chitosan was more hydrophilic in nature. In agreement with the DSC data, the TGA (Fig. 3b) indicated that the TGA-CMC-CD(1) started to degrade at lower temperature (215 °C) compared to the pristine chitosan (240 °C). This can be ascribed to both the presence of easily breakable side chains (due to $-NH–CO–CH_2–SH$ formation) in the TGA-CMC-CD(1) structure and the amorphous state of this polymer [14].

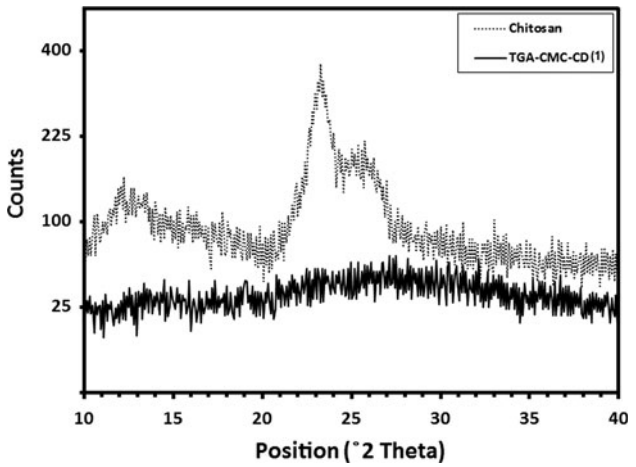

Fig. 2 XRD patterns for chitosan and TGA-CMC-CD(1) samples

4.2 Characterization of the prepared nanoparticles (free and albendazole-loaded nanoparticles)

The formation of chitosan-based polymer/TPP nanoparticles occurs spontaneously upon incorporation of the negatively charged TPP into the chitosan derivative solution because of the complexation between oppositely charged species. The process of formation of complexes is very simple and mild, avoiding possible toxicity of chemical reagents and other undesirable effects [12].

The size and morphology of the prepared nanoparticles were investigated by SEM. Fig. 4 represents the SEM images along with particle size distributions (Fig. 4a–d, right column) of the TGA-CMC-CD(1) nanoparticles, prepared using aqueous solutions containing different TPP loadings. Figure 4e shows the mean diameter (D) of the TGA-CMC-CD(1) nanoparticles versus TPP concentration, as deduced from the histograms in Fig. 4a–d. Although, one may expect D to decrease monotonically with TPP concentration, Fig. 4e demonstrates D increased from a value of around 50 nm at a TPP concentration of 1 wt% to a value of around 60 nm at a TPP concentration of 2 wt%. Therefore, there was an optimal TPP concentration (1 wt%, here) at which nanoparticles with the smallest size were formed. Investigation of the polydispersity index (PDI) of each nanoparticle system, displayed as insets of Fig. 4a–d (right column), revealed that the most uniform particles (with the smallest PDI value) were also obtained at the same TPP concentration (1 wt%). Actually, at TPP concentrations lower than 1 wt%, the number of TPP molecules was insufficient to create nanoparticles as small as those which were created by a TPP concentration of 1 wt%. On the other hand, excess amounts of TPP (TPP

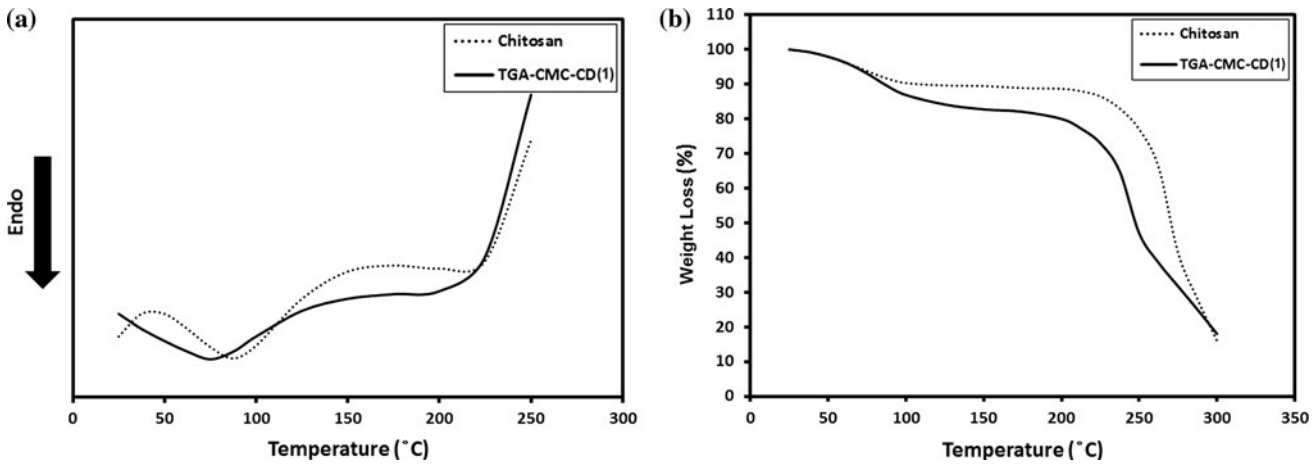

Fig. 3 **a** DSC thermograms and **b** TGA curves of chitosan and TGA-CMC-CD(1) samples

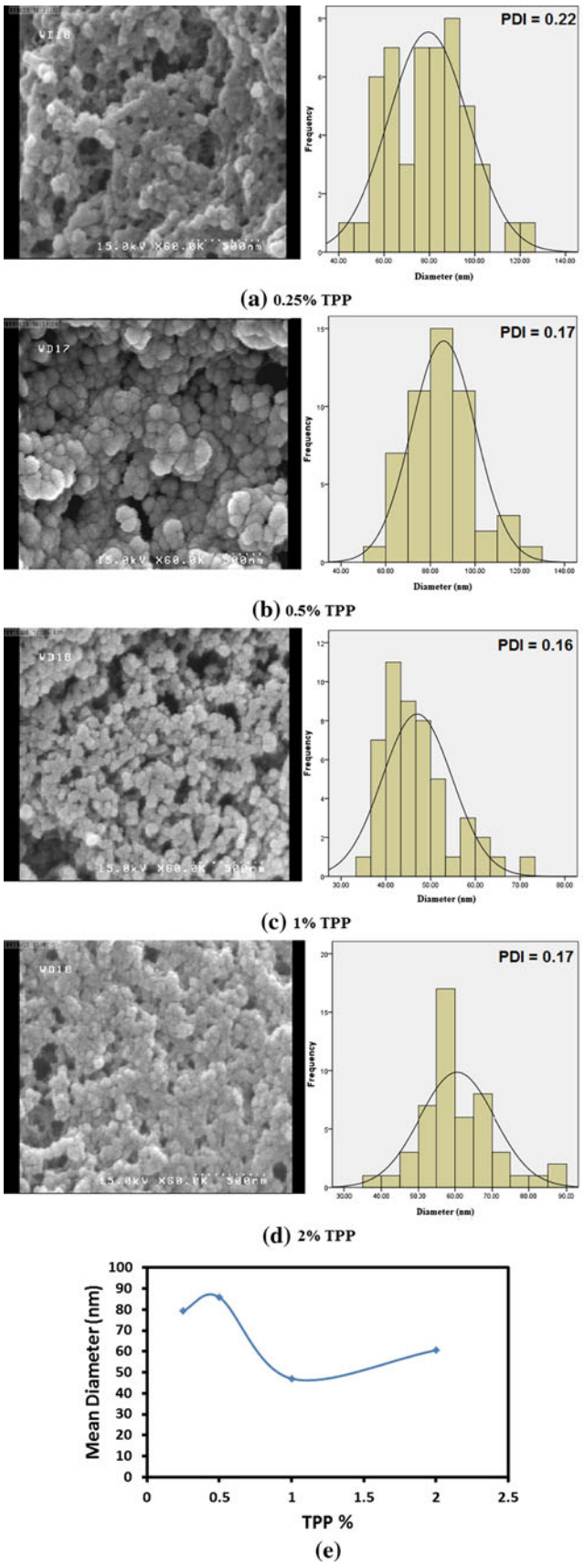

◀ **Fig. 4** **a–d** SEM images (*left column*) and size distributions (*right column*) of TGA-CMC CD(1) nanoparticles prepared using aqueous solutions containing different concentrations of TPP. **e** Mean diameter (D) of TGA-CMC-CD(1) nanoparticles versus TPP concentration

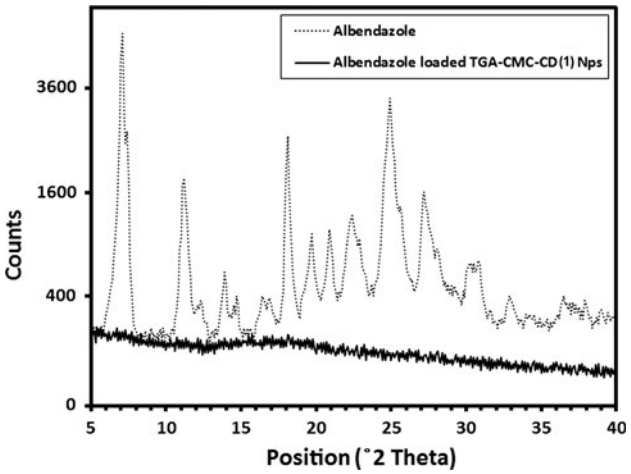

Fig. 5 XRD patterns of albendazole and albendazole-loaded TGA-CMC-CD(1) nanoparticles

concentrations higher than 1 wt%), led to more TGA-CMC-CD(1) molecules involved in the formation of a single nanoparticle, resulting in a larger particle size [31]. Accordingly, aqueous solutions containing 1 wt% of the TPP were used for the preparation of free and albendazole loaded nanoparticles for the following investigations.

Figure 5 demonstrates the X-ray diffraction patterns of the albendazole and albendazole-loaded TGA-CMC-CD(1) nanoparticles. There were several sharp crystal peaks in the XRD pattern of albendazole as a highly crystalline material. These peaks disappeared in the XRD pattern of the albendazole-loaded nanoparticle, due to the possible overlapping of the peaks with the noise of the coated polymer. Also, albendazole could form an amorphous complex with TGA-CMC-CD matrix, resulting in the typical pattern of non-crystalline materials.

The DSC thermograms of pure albendazole, as well as unloaded and albendazole-loaded TGA-CMC-CD(1) nanoparticles are shown in Fig. 6a. Albendazole exhibited a sharp endothermic melting peak at 220 °C. This characteristic peak disappeared after encapsulation of albendazole in the nanoparticles, indicating the amorphous dispersion of the drug in the nanoparticles [32, 33].

Figure 6b shows the TGA curves of albendazole, TGA-CMC-CD(1) nanoparticles and albendazole-loaded TGA-CMC-CD(1) nanoparticles. The observed transition around 100 °C was attributed to the loss of water from the TGA-CMC-CD(1) nanoparticles. Although, the main degradation of pure albendazole occurred around 270 °C, unloaded

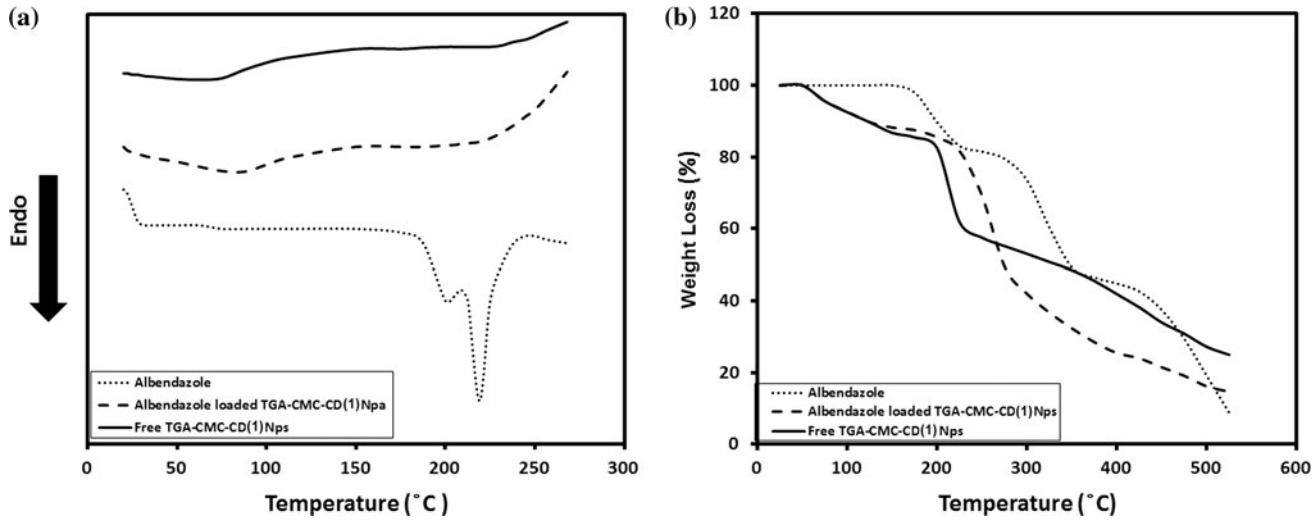

Fig. 6 **a** DSC thermograms and **b** TGA curves of albendazole, free TGA-CMC-CD(1) and albendazole-loaded TGA-CMC-CD(1) nanoparticles

and albendazole-loaded TGA-CMC-CD(1) nanoparticles started to degrade at 200 and 230 °C, respectively. Therefore, the improved thermal stability of the loaded TGA-CMC-CD(1) nanoparticles compared to the unloaded ones could be due to the dispersion of albendazole in the former nanoparticles. Combining the results of XRD and DSC/TGA, it is reasonable to conclude that albendazole was successfully encapsulated into the core of the TGA-CMC-CD(1) nanoparticles.

4.3 Mucoadhesion studies

Various authors have suggested that rheological characterization of a polymer–mucin mixture can provide an acceptable in vitro model representative of the true in vivo mucoadhesive properties of the polymer [34, 35]. In other words, a mixture containing nanoparticles with strong mucoadhesive properties is expected to have a greater storage modulus compared to the one containing nanoparticles with a weak mucoadhesion ability. Therefore, rheological investigations were performed to examine the mucoadhesive properties of chitosan, TGA-CMC-CD (1) and TGA-CMC-CD (2) nanoparticles. Figure 7a shows the frequency dependence of storage (G′) and loss (G″) modulus for freshly made chitosan/mucin, TGA-CMC-CD(1)/mucin and TGA-CMC-CD(2)/mucin solutions. G″ values of each solution were larger than the corresponding G′ values in entire studied frequency range, indicating that weakly entangled viscoelastic solutions were formed in the original state of preparation. In the case of chitosan nanoparticles, G′ values decreased in the high frequency region. This was attributed to the absence of thiol groups in the pristine chitosan structure, resulting in weak mucoadhesive properties. On the other hand, the values of storage modulus (G′) of the TGA-CMC-CD(1)/mucin and TGA-CMC-CD(2)/mucin mixtures increased with frequency in the high frequency region, due to the formation of disulfide bonds between the polymers and mucin.

In order to further elucidate the differences between mucoadhesive properties of the pristine and thiolated chitosans, the freshly made solutions of chitosan/mucin, TGA-CMC-CD(1)/mucin and TGA-CMC-CD(2)/mucin were rested for 30 min at room temperature and then their G' versus frequency behaviors were compared, Fig. 7b. The storage modulus versus frequency plot of the chitosan/mucin solution in Fig. 7b was the same as that of the chitosan/mucin solution in Fig. 7a. However, G′ values of the TGA-CMC-CD(1)/mucin and TGA-CMC-CD(2)/mucin solutions, after resting for 30 min, were enhanced compared to those of the freshly made ones, due to the increase of the number of disulfide bonds between the thiolated polymers and mucin after 30 min. In addition, G′ values of the rested TGA-CMC-CD(1)/mucin and TGA-CMC-CD(2)/mucin solutions became frequency independent, indicating strong interactions between the thiolated chitosans and mucin [36]. Finally, the TGA-CMC-CD(1)/mucin solution, showed enhanced modulus compared to the TGA-CMC-CD(2)/mucin one, which was attributed to the higher amount of the immobilized thiol groups on the TGA-CMC-CD(1) polymer.

4.4 Drug loading and release studies

Although albendazole has been proven to be an effective drug in the treatment of several parasitic diseases and cancer [37], studies devoted to its release profile from nanocarriers are scarce in open literature. Therefore, as one of the objectives of this research, we investigated the

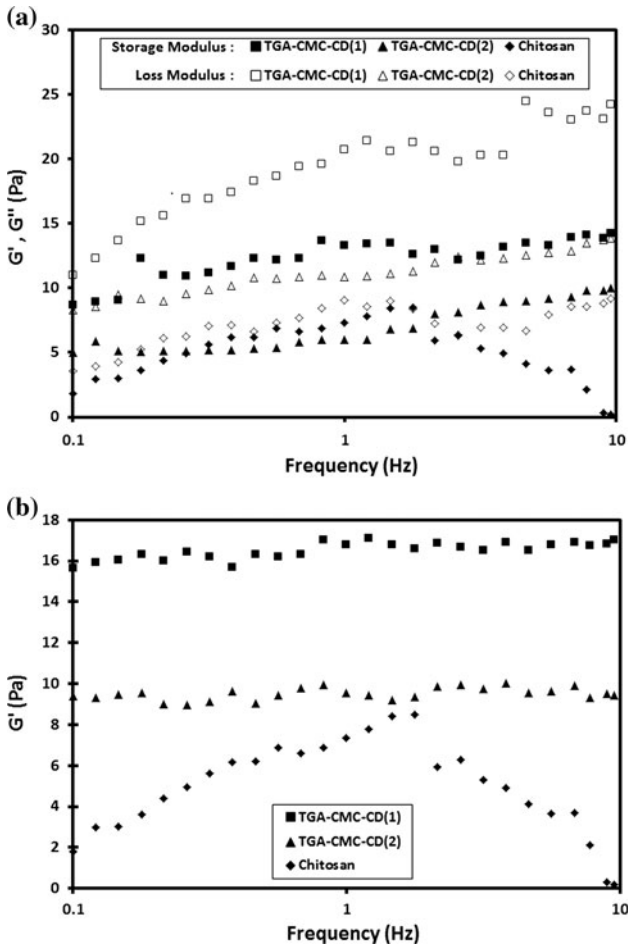

Fig. 7 **a** frequency dependence of storage, G′, (*filled square*, *filled triangle*, *filled diamond*) and loss, G″ (*open square*, *open triangle*, *open diamond*) modulus for freshly made chitosan/mucin, TGA-CMC-CD(1)/mucin and TGA-CMC-CD(2)/mucin solutions **(b)** frequency dependence of G'for chitosan/mucin, TGA-CMC-CD(1)/mucin and TGA-CMC-CD(2)/mucin solutions, after resting for 30 min at room temperature

in vitro release of albendazole from the prepared nanoparticles.

Albendazole entrapment efficiencies (EE) of the nanoparticles are reported in Table 1. Pristine chitosan contained the least amount of albendazole, since it lacked necessary functional groups to interact with this hydrophobic drug. On the other hand, entrapment efficiencies of the nanoparticles were increased up to 10 % by introducing cyclodextrin to the chitosan structure. Inspection of the data of Table 1 reveals that EEs of the TGA-CMC-CD nanoparticles were increased by increasing the amount of the coupled thiol groups. Therefore, increased amount of thiol groups not only improved the nanoparticles mucoadhesive properties (as described in the previous section), but also their albendazole entrapment efficiency.

Since, it has been shown that consideration of partial solubility parameters can be used to accurately predict polymer–drug miscibility or compatibility [30, 38], an effort was made to gain a quantitative understanding of the extent of the chitosan-based polymers/albendazole compatibilies by calculating the solubility parameters of the polymers and drug as well as the polymers/albendazole mixing enthalpy (ΔH_m(, Sect. 2.8. Table 1 summarizes the partial solubility parameter values, calculated by the group contribution method, Eq. (2), for albendazole, chitosan, CMC-CD, TGA-CMC-CD(1) and TGA-CMC-CD(2). Also the values of ΔH_m calculated by Eq. (3), for various polymer/drug systems are included in Table 1. Due to the fact that compatibility and miscibility between two phases of a mixture are inversely proportional to their ΔH_m value [39–41], one could conclude, based on the data of Table 1, that among the samples tested, TGA-CMC-CD(1) was able to encapsulate the greatest amount of albendazole. Interestingly, this theoretical prediction was in agreement with the experiment, where TGA-CMC-CD(1) nanoparticles were also found to have the highest drug entrapment efficiency (Table 1). It should be noted that this approach was recently used by Kim et al. [38] to synthesize block copolymer micelles as a potential delivery system for albendazole.

Figure 8 demonstrates the cumulative release profiles for the albendazole-loaded nanoparticles as a function of time. The release profiles from the modified and un-modified nanoparticles followed a similar trend: an initial rapid release in the first 10 h and a slow and steady release in the following period. However, there were some significant differences among the profiles of Fig. 8 that could serve to provide useful information on the role of the degree of polymer/drug compatibility on the drug release from the nanoparticles. As can be viewed, nanoparticles of the most incompatible polymer, chitosan, allowed 85 % release of albendazole within the first 10 h, while nanoparticles based on the more compatible polymers, TGA-CMC-CD(1) and TGA-CMC-CD(2), released 70 and 78 % of the entrapped drug, respectively, in the first 10 h. Moreover, 100 % albendazole release was observed after 130, 170 and 168 h from the chitosan, TGA-CMC-CD(1) and TGA-CMC-CD(2) nanoparticles, respectively. The above profiles are comparable with albendazole release behavior of other types of carriers such as block copolymer micelles [38] and PEGylated liposomes [42] and show the potential of the modified chitosan nanoparticles as sustained albendazole delivery systems. The results are also consistent with the fact that the higher the compatibility between a polymer and a drug is, the slower should be the release of the drug from the nanoparticles composed of the polymer. Although, due to the higher ΔH_m value of the CMC-CD/albendazole mixture than that of the TGA-CMC-CD(1)/albendazole one, CMC-CD nanoparticles were expected to release more albendazole than TGA-CMC-CD(1)

Table 1 Albendazole entrapment efficiency along with three-dimensional solubility parameters and molar volumes of albendazole and various polymer systems and ΔH_m values of polymer/albendazole binary mixtures

System	EE (%)	δ_d $MPa^{0.5}$	δ_p $MPa^{0.5}$	δ_h $MPa^{0.5}$	V cm^3/mole	ΔH_m (polymer/albendazole) MPa
Albendazole	–	18.90	7.40	3.60	203.10	–
Chitosan	23	22.90	17.20	25.90	80.50	100.10
CMC-CD	32	16.74	6.22	16.18	267.30	25.40
TGA-CMC-CD(1)	33	16.80	6.21	16.19	267.50	25.03
TGA-CMC-CD(2)	29	16.70	6.20	16.18	267.70	26.04

The solubility parameters and molar volumes of albendazole and chitosan were cited from Refs. [38] and [39] respectively, while those of the CMC-CD, TGA-CMC-CD(1) and TGA-CMC-CD(2) were estimated by the group contribution method [29], considering the structure of their repeating units, depicted in Scheme 1

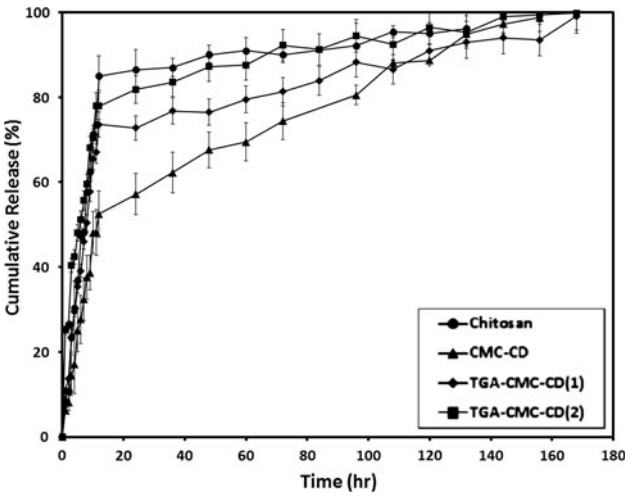

Fig. 8 Release kinetics of albendazole from the prepared nanoparticles (the *solid lines* are guides to eye)

nanoparticles, they released only 53 % of the drug within the first 10 h. This discrepancy is believed to be caused by the high cross-linking density of the CMC-CD network, originated from a large number of reactions between free amino groups of the CMC-CD polymer and the TPP counterion during the formation of the CMC-CD nanoparticles. Actually, an increase in the CMC-CD nanoparticles cross-linking density caused an increase in the glass transition temperature (T_g) of the CMC-CD chains, leading to restriction of drug mobility in the core of the nanoparticles.

5 Conclusions

TGA-CMC-CD nanoparticles were synthesized by an ionic-gelation method using TPP as the gelling counter ion, for mucosal albendazole delivery applications. The use of HMDI during immobilization of CD onto CMC allowed the interaction of CD molecules with the provided active sites at the C_6-position of chitosan. Therefore, amino groups of chitosan at the C_2-position remained free to form amide bonds with TGA molecules and TPP in the subsequent gelation process. XRD and DSC/TGA measurements revealed the ability of the nanoparticles to encapsulate the drug successfully. Rheological studies showed that increasing the amount of grafted thiol groups on the nanoparticles improved their mucoadhesive properties. Also, nanoparticles containing the highest amount of immobilized thiol groups and being prepared using an aqueous solution containing 1 wt% of TPP, TGA-CMC-CD(1), were found to be the most suitable carriers for albendazole, since they exhibited the highest drug entrapment efficiency as well as the slowest and most steady release profile. The high affinity of the TGA-CMC-CD(1) polymer to albendazole was explained theoretically by calculating the polymer/albendazole mixing enthalpy using the group contribution method.

References

1. Min KH, Park K, Kim YS, Bae SM, Lee S, Jo HG, Park RW, Kim IS, Jeong SY, Kim K, Kwon IC. Hydrophobically modified glycol chitosan nanoparticles-encapsulated camptothecin enhance the drug stability and tumor targeting in cancer therapy. J Controlled Release. 2008;127:208–18.
2. Navarrete-Vazquez G, Yepez L, Hernandez-Campos A, Tapia A, Hernandez-Luis F, Cedillo R, Gonzalez J, Martinez-Fernandez A, Martinez-Grueiro M, Castillo R. Synthesis and antiparasitic activity of albendazole and mebendazole analogues. Bioorg Med Chem. 2003;11:4615–22.
3. Letchford K, Burt H. A review of the formation and classification of amphiphilic block copolymer nanoparticulate structures: micelles, nanospheres, nanocapsules and polymersomes. Eur J Pharm Biopharm. 2007;65:259–69.
4. Hamidi M, Azadi A, Rafiei P. Hydrogel nanoparticles in drug delivery. Adv Drug Delivery Rev. 2008;60:1638–49.
5. Aliaghaie M, Mirzadeh H, Dashtimoghadam E, Taranejoo Sh. Investigation of gelation mechanism of an injectable hydrogel based on chitosan by rheological measurements for a drug delivery application. Soft Matter. 2012;8:3128–37.

6. Fattal E, Pecquet S, Couvreur P, Andremont A. Biodegradable microparticles for the mucosal delivery of antibacterial and dietary antigens. Int J Pharm. 2002;242:15–24.
7. Liu W, Wu W, Selomulya C, Chen XD. A single step assembly of uniform microparticles for controlled release applications. Soft Matter. 2011;7:3323–30.
8. Rieux A, Fievez V, Garinot M, Schneider YJ, Préat V. Nanoparticles as potential oral delivery systems of proteins and vaccines: a mechanistic approach. J Controlled Release. 2006;116: 1–27.
9. Raemdonck K, Demeester J, De Smedt S. Advanced nanogel engineering for drug delivery. Soft Matter. 2009;5:707–15.
10. Dash M, Chiellini F, Ottenbrite RM, Chiellini E. Chitosan—A versatile semi-synthetic polymer in biomedical applications. Prog Polym Sci. 2011;36:981–1014.
11. Taranejoo Sh, Janmaleki M, Rafienia M, Kamali M, Mansouri M. Chitosan microparticles loaded with exotoxin A subunit antigen for intranasal vaccination against Pseudomonas aeruginosa: an in vitro study. Carbohydr Polym. 2011;83:1854–61.
12. Saboktakin MR, Tabatabaie RM, Maharramov A, Ramazanov MA. Synthesis and characterization of pH-dependent glycol chitosan and dextran sulfate nanoparticles for effective brain cancer treatment. Int J Biol Macromol. 2011;49:747–51.
13. Alves NM, Mano JF. Chitosan derivatives obtained by chemical modifications for biomedical and environmental applications. Int J Biol Macromol. 2008;43:401–14.
14. Anitha A, Maya S, Deepa N, Chennazhi KP, Nair SV, Tamura H, Jayakumar R. Efficient water soluble *O*-carboxymethyl chitosan nanocarrier for the delivery of curcumin to cancer cells. Carbohydr Polym. 2011;83:452–61.
15. Molnar E, Barbu E, Lien ChF, Gorecki DC, Tsibouklis J. Toward drug delivery into the brain: synthesis, characterization, and preliminary in vitro assessment of alkylglyceryl-functionalized chitosan nanoparticles. Biomacromolecules. 2010;11:2880–9.
16. Prabaharan M, Grailer JJ, Steeber DA, Gong Sh. Stimuli-responsive chitosan-graft-poly(*N*-vinylcaprolactam) as a promising material for controlled hydrophobic drug delivery. Macromol Biosci. 2008;8:843–51.
17. Krauland AH, Alonso MJ. Chitosan/cyclodextrin nanoparticles as macromolecular drug delivery system. Int J Pharm. 2007;340: 134–42.
18. Prabaharan M, Mano JF. Chitosan derivatives bearing cyclodextrin cavitiesas novel adsorbent matrices. Carbohydr Polym. 2006;63:153–66.
19. Ping Y, Liu C, Zhang Z, Liu KL, Chen J, Li J. Chitosan-graft-(PEI-β-cyclodextrin) copolymers and their supramolecular PEGylation for DNA and siRNA delivery. Biomaterials. 2011; 32:8328–41.
20. Peng K, Tomatsu I, Korobko AV, Kros A. Cyclodextrin–dextran based in situ hydrogel formation: a carrier for hydrophobic drugs. Soft Matter. 2010;6:85–7.
21. Davis ME, Brewster ME. Cyclodextrin-based pharmaceutics: past, present and future. Nat Rev Drug Discovery. 2004;3: 1023–35.
22. Prabaharan M, Gong Sh. Novel thiolated carboxymethyl chitosan-g-β-cyclodextrin as mucoadhesive hydrophobic drug delivery carriers. Carbohydr Polym. 2008;73:117–25.
23. Torrado S, Lopez ML, Torrado G, Bolas F, Torrado S, Cadorniga R. A novel formulation of albendazole solution: oral bioavailability and efficacy evaluation. Int J Pharm. 1997;156:181–7.
24. Leonardi D, Lamas MC, Olivieri AC. Multiresponse optimization of the properties of albendazole-chitosan microparticles. J Pharm Biomed Anal. 2008;48:802–7.
25. Chiu SH, Chung TW, Giridhar R, Wu WT. Immobilization of b-cyclodextrin in chitosan beads for separation of cholesterol from egg yolk. Food Res Int. 2004;37:217–23.
26. Saboktakin MR, Tabatabaie RM, Maharramov A, Ramazanov MA. Development and in vitro evaluation of thiolated chitosan—Poly(methacrylic acid) nanoparticles as a local mucoadhesive delivery system. Int J Biol Macromol. 2011;48(3):403–7.
27. Shahnaz G, Perera G, Sakloetsakun D, Rahmat D, Bernkop-Schnürch A. Synthesis, characterization, mucoadhesion and biocompatibility of thiolated carboxymethyl dextran-cysteine conjugate. J Controlled Release. 2010;144:32–8.
28. Anitha A, Deepa N, Chennazhi KP, Nair SV, Tamura H, Jayakumar R. Development of mucoadhesive thiolated chitosan nanoparticles for biomedical applications. Carbohydr Polym. 2011;83:66–73.
29. Van Krevelen DW. Properties of polyzmers. 3rd ed. Amsterdam: Elsevier; 1990.
30. Liu J, Xiao Y, Allen Ch. Polymer–drug compatibility: a guide to the development of delivery systems for the anticancer agent, ellipticine. J Pharm Sci. 2004;93:132–43.
31. Fana W, Yanb W, Xub Z, Ni H. Formation mechanism of monodisperse, low molecular weight chitosan nanoparticles by ionic gelation technique. Colloids Surf B: Biointerfaces. 2012; 90:21–7.
32. Saremi S, Atyabi F, Akhlaghi SP, Ostad SN, Dinarvand R. Thiolated chitosan nanoparticles for enhancing oral absorption of docetaxel: preparation, in vitro and ex vivo evaluation. Int J Nanomedicine. 2011;6:119–28.
33. Mahmoud AA, El-Feky GS, Kamel R, Awad GhEA. Chitosan/sulfobutylether-β-cyclodextrin nanoparticles as a potential approach for ocular drug delivery. Int J Pharm. 2011;413:229–36.
34. Riley R, Smart J, Tsibouklis J, Dettmar P, Hampson F, Davis JA, Kelly G, Wilber W. An investigation of mucus/polymer rheological synergism using synthesised and characterised poly (acrylic acid)s. Int J Pharm. 2001;217:87–100.
35. Andrews GP, Laverty TP, Jones DS. Mucoadhesive polymeric platforms for controlled drug delivery. Eur J Pharm Biopharm. 2009;71:505–18.
36. Sakloetsakun D, Hombach JMR, Bernkop-Schnürch A. In situ gelling properties of chitosan-thioglycolic acid conjugate in the presence of oxidizing agents. Biomaterials. 2009;30:6151–6.
37. Venkatesan P. Albendazole. J Antimicrob Chemother. 1998;41: 145–7.
38. Kim Y, Pourgholami MH, Morris DL, Stenzel MH. An Optimized RGD-decorated micellar drug delivery system for albendazole for the treatment of ovarian cancer: from RAFT polymer synthesis to cellular uptake. Macromol Biosci. 2011;11:219–33.
39. Ravindra R, Krovvidi KR, Khan AA. Solubility parameter of chitin and chitosan. Carbohydr Polym. 1998;36:121–7.
40. Icoz DZ, Kokini JL. Quantitative prediction of molecular miscibility in dextran systems as model carbohydrate polymers. Carbohydr Polym. 2007;70:181–91.
41. Icoz DZ, Kokini JL. Theoretical analysis of predictive miscibility of carbohydrate polymers—Software calculations for inulin–amylopectin systems. Carbohydr Polym. 2008;72:5205–9.
42. Panwar P, Pandey B, Lakhera PC, Singh KP. Preparation, characterization, and in vitro release study of albendazole-encapsulated nanosize liposomes. Int J Nanomedicine. 2010;5:101–8.